



## ISTITUTO NAZIONALE DI RICERCA METROLOGICA Repository Istituzionale

### Prediction of Energy Losses in Soft Magnetic Materials Under Arbitrary Induction Waveforms and DC Bias

This is the author's accepted version of the contribution published as:

*Original*

Prediction of Energy Losses in Soft Magnetic Materials Under Arbitrary Induction Waveforms and DC Bias / de la Barrière, Olivier; Ragusa, Carlo; Appino, Carlo; Fiorillo, Fausto. - In: IEEE TRANSACTIONS ON INDUSTRIAL ELECTRONICS. - ISSN 0278-0046. - 64:2(2017). [10.1109/TIE.2016.2608886]

*Availability:*

This version is available at: 11696/54694 since: 2021-02-07T06:29:17Z

*Publisher:*

IEEE

*Published*

DOI:10.1109/TIE.2016.2608886

*Terms of use:*

This article is made available under terms and conditions as specified in the corresponding bibliographic description in the repository

*Publisher copyright*

IEEE

© 20XX IEEE. Personal use of this material is permitted. Permission from IEEE must be obtained for all other uses, in any current or future media, including reprinting/republishing this material for advertising or promotional purposes, creating new collective works, for resale or redistribution to servers or lists, or reuse of any copyrighted component of this work in other works

(Article begins on next page)

# Prediction of Energy Losses in Soft Magnetic Materials Under Arbitrary Induction Waveforms and DC Bias

Olivier de la Barrière, Carlo Ragusa, *Member, IEEE*, Carlo Appino, and Fausto Fiorillo

**Abstract**—The Statistical Theory of Losses (STL) provides a simple and general method for the interpretation and prediction of the energy losses in soft magnetic materials. One basic application consists, for example, in the prediction of the loss under arbitrary induction waveform, starting from data available from conventional measurements performed under sinusoidal flux. There are, however, persisting difficulties in assessing the loss when the induction waveform is affected by a DC-bias, because this would require additional experimental data, seldom available to machine designers. In this paper we overcome this problem applying, with suitable simplifications, the dynamic Preisach model. Here the parameters of the STL model are obtained exploiting preemptive conventional measurements only. By this new simplified method, analytical expressions for the loss components are obtained under general supply conditions, including DC-biased induction waveforms.

**Index Terms**—Magnetic hysteresis, magnetic loss, magnetic materials.

## I. INTRODUCTION

THE optimal design of magnetic components like electrical machines or power electronics transformers in modern applications, e.g. renewable energy production [1] or hybrid traction [2], can be quite a complex task. It often requires the optimization of the electrical machine under complex constraints, with a significant number of working points to be satisfied in the torque vs. speed plan [3]. In embedded applications the torque density [4] is a crucial objective, while it is often necessary to simultaneously maximize the efficiency

[5] [6]. These multi-objective design problems often require the use of stochastic algorithms, such as evolutionary [7] or particles swarm algorithms [8] [9], to overcome the problem of local extrema of the global objective function [10]. They generally call for a huge number of model evaluations for converging to the optimal solution and the electromagnetic model implemented in the optimization process must offer the best compromise between accuracy and computation time.

In this context, iron loss modeling plays a crucial role, because it has a direct impact on the machine efficiency [11] [12]. The loss calculation is a complex problem, often made more demanding by specific working regimes, where, for example, the induction waveform is distorted or affected by a DC-bias, an ubiquitous circumstance in electrical engineering [13][14]. The relevance of DC-biased and asymmetric inductions in power electronics has also been pointed out [15] and the important case of Pulse Width Modulation (PWM) [16] can also be seen as a problem of polarized induction waveform. Indeed, the main difficulty arising with PWM waveforms is the prediction of the loss associated with minor loops. Each of these minor loops can be considered as a DC-biased cycle of small peak-to-peak amplitude [17]. For electrical machine designers, DC-biased inductions waveforms are mostly found in the rotor of electrical machines. To illustrate this point, let us consider a synchronous permanent magnet machine, which is interesting in hybrid vehicles due to its high torque density [18]. The machine has two pole pairs and non-salient rotor (Fig.1). We are interested in the no-load magnetic flux density in the ferromagnetic rotor (which is in many cases made of laminated material). Fig. 1. shows that the radial induction waveform at a given point of the rotor yoke (obtained, for example, with a finite-element computation) is affected by a DC-bias, with superposed undulation. The bias is generated by the permanent magnets and the oscillation around it is the effect of machine slotting. The space and time harmonics of the stator magnetomotive force can also be responsible for variations of the rotor induction around the DC-bias value [19]. In low cost machines with concentrated windings, it may happen that the rotor loss provides the larger contribution to the iron loss [20], while becoming crucial from the thermal viewpoint, because of the difficulty to cool the rotor.

In the literature, three classes of loss models can be found, each of them offering a different compromise between accuracy and computational complexity [21].

Manuscript received March 14, 2016; revised June 10, 2016 and July 15, 2016; accepted August 3, 2016.

O. de la Barrière is with SATIE, ENS Cachan, CNRS, UniverSud, 61 av. du Président Wilson, F-94230 Cachan, France (e-mail: olivier.de-la-barriere@satie.ens-cachan.fr).

C. Ragusa is with Energy Department, Politecnico di Torino, Corso Duca degli Abruzzi 24, 10129 Torino, Italy (corresponding author, phone: +39 011 0907 153, fax: +39 011 0907 199, e-mail: carlo.ragusa@polito.it).

C. Appino and F. Fiorillo are with Istituto Nazionale di Ricerca Metrologica (INRiM), Strada delle Cacce 91, 10135 Torino, Italy (e-mail: appino@inrim.it, f.fiorillo@inrim.it).

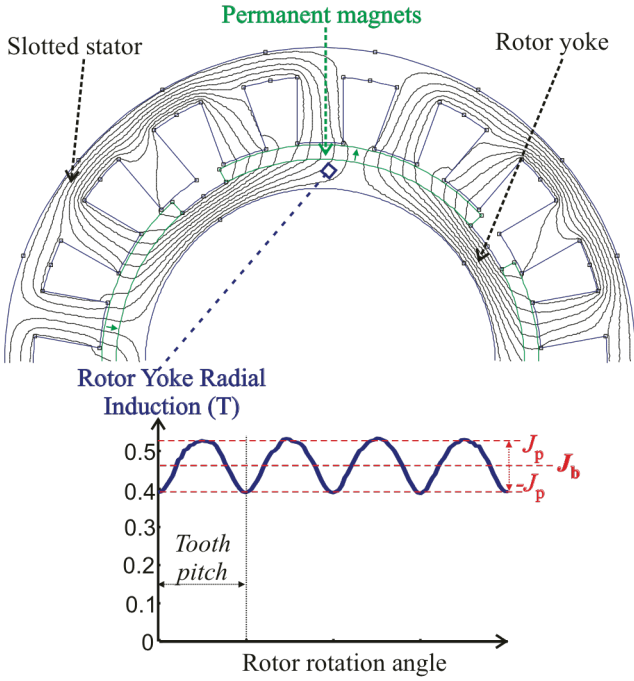


Fig. 1. Radial induction waveform in the rotor yoke of a permanent magnet machine.

The phenomenological models derived from the old Steinmetz formula are often used in electrical engineering [22]. Mostly limited to conventional supply conditions, they consist of fast and simple analytical expressions giving the specific power loss as a function of frequency and peak induction. Authors in [23] have proposed suitable modifications of the Steinmetz equation to account for the induction distortion and the DC-bias. Experimental aspects of the loss behavior of DC-biased loops have been discussed in [24] [25]. A two-term loss formulation was proposed in [26], where the first term represents the classical contribution, proportional (in terms of power) to  $(B_p f)^2$ , with  $B_p$  the peak induction, while the second term, proportional to  $B_p^2 f$ , takes into account the DC bias contribution.

A second type of approach is based on the Dynamic Preisach Model (DPM) [27], which can predict the loss under generic induction waveform, including distorted and DC-biased waveform with and without minor loops. With suitable generalization, the DPM can take into account the skin effect [28], but, as shown in [28] [29], this fully numerical modeling requires heavy calculations, because it is necessary to compute at each instant of time the state of each switching Preisach unit. Recently, however, a simple differential equation describing the dynamic effects of the hysteresis through suitable simplification of the DPM has been proposed [30] [31]. This approach has the advantage of predicting the hysteresis loop and the related loss with good accuracy, close to the one provided by the DPM, but with a largely reduced computational effort.

The third class of models is based on the Statistical Theory of Losses (STL) [32] [33]. By this theory, the loss per cycle  $W$  under whatever induction waveform is decomposed at any frequency as:

$$W = W_h + W_{cl} + W_{exc}, \quad (1)$$

where  $W_h$  is the hysteresis (quasi-static) loss,  $W_{cl}$  is the classical loss and  $W_{exc}$  is the excess loss. Following this approach, the classical energy loss component can be computed by the standard equation (valid under negligible skin effect) [33]:

$$W_{class} = \sigma \frac{d^2}{12} \int_0^{1/f} \left( \frac{dB}{dt} \right)^2 dt, \quad (2)$$

where  $\sigma$  is the material electrical conductivity,  $d$  is the sheet thickness,  $f$  the magnetizing frequency, and  $B(t)$  the instantaneous flux density. Since only the time derivative  $dB/dt$  is involved in (2),  $W_{class}$  does not depend on the DC-bias, which influences instead the hysteresis and excess components. The latter can be written as:

$$W_{exc} = \sqrt{\sigma G S V_0} \cdot \int_0^{1/f} \left| \frac{dJ}{dt} \right|^{3/2} dt, \quad (3)$$

where  $J$  is the magnetic polarization ( $J = B - \mu_0 H$ ),  $S$  is the cross-sectional area of the lamination,  $G = 0.1356$  is a dimensionless coefficient, and  $V_0$  is a statistical parameter, related to the distribution of the local coercive fields, which depends on the peak induction  $B_p$  and the bias induction  $B_b$ . The authors of [34] [35] have applied the Static Preisach Model (SPM) to compute  $W_{hyst}$ , but their simplified model neglects the  $W_{exc}$  dependence on the DC-bias. The structure dependent  $V_0$  parameter, in particular, is assumed to be equal to the one belonging to the centered hysteresis loop of identical peak-to-peak amplitude, an hypothesis also exploited for the minor loops associated with PWM waveforms [17]. It has been shown that this approximation does not introduce in general important errors, because the excess loss is only a part of the total loss, but it is not physically justified.

This limitation is overcome in this paper, where, by suitable implementation of the simplified DPM [30] [31], it is possible to predict in fast and simple way the loss evolution with the DC bias by predicting the corresponding evolution of the parameters of the STL. It offers an excellent tradeoff between the computation time and the accuracy.

The effect of a DC-bias induction is addressed experimentally, and the theory here outlined is applied to several experimental results obtained on non-oriented and grain-oriented iron-silicon laminations.

## II. THEORETICAL MODEL

We start from a simple dynamical model of hysteresis, introduced in [31] where the relation between the dynamic field  $H(t)$  and the magnetic polarization  $J(t)$  is decomposed into a dynamic part and a static part. This model is sketched in Fig. 2, where we introduce the *static field*  $H_{stat}(t)$ , which is defined as the field providing a given magnetic polarization

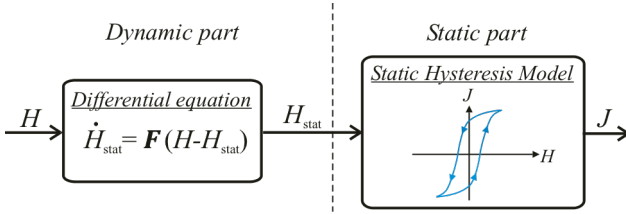


Fig. 2. Block diagram of the dynamic model.

value under quasi-static conditions. The static field  $H_{stat}(t)$  is obtained from the dynamic field  $H(t)$  (step 1 in Fig. 2) and the polarization  $J(t)$  is subsequently computed via the Static Hysteresis Model. As discussed in [31], the following dynamic equation relates  $H(t)$  and  $H_{stat}(t)$

$$\dot{H}_{stat} = \text{sign}[H(t) - H_{stat}(t)] \frac{9}{16} k_d [H(t) - H_{stat}(t)]^2, \quad (4)$$

where  $k_d$  is a suitable parameter governing the dynamics of the magnetization reversal [27]. From (4) we obtain the dynamic field  $H(t)$  as

$$H(t) = H_{stat}(t) + \text{sign}(\dot{H}_{stat}) \cdot \frac{4}{3} \sqrt{\frac{|\dot{H}_{stat}|}{k_d}}. \quad (5)$$

The second term on the right hand side of (5) is the excess field  $H_{exc} = H - H_{stat}$ , which depends on the time derivative of the static field  $H_{stat}$ . Equation (5) brings then the dynamic field back to the static one, which can in turn be related to the polarization  $J(t)$  by means of the Static Preisach Model (SPM). By this model, one finds that for a generic hysteresis cycle taken between  $H_m$  and  $H_M$ , the descending branch  $J_d$  of the given cycle can be computed according to

$$J_d = F(H_M, -H_M) - 2 \cdot F(H_M, H_{stat}), \quad (6)$$

where  $F(\alpha, \beta)$  is the Everett's function [36],  $H_m$  and  $H_M$  are the fields required to reach, under static conditions, the lower and upper value of the polarization waveform, and  $H_m \leq H_{stat} \leq H_M$ . The condition  $|H_m| \leq H_M$  is posed, implying positive DC bias. A similar equation applies for the ascending branch,  $J_a$ :

$$J_a = F(H_M, -H_M) - 2 \cdot F(H_M, H_m) + 2 \cdot F(H_{stat}, H_m). \quad (7)$$

In the following we shall apply the method discussed in [36], where the Everett's function is computed on the basis of the minimum preemptive experimental data provided by the *limit* (very high peak induction) experimental cycle. Following [33], the function  $F(\alpha, \beta)$  for generic switching fields  $\alpha$  and  $\beta$  in the Preisach plane is obtained as

$$F(\alpha, \beta) = -\frac{1}{2} J_{d,lim}(-\alpha) - \frac{1}{2} J_{d,lim}(\beta) + \Phi(\alpha) \cdot \Phi(-\beta), \quad (8)$$

where  $J_{d,lim}(\alpha)$  represents the descending branch of the experimental *limit cycle* and  $\Phi$  is the function

$$\Phi(H_{stat}) = -\sqrt{J_{d,lim}(0)} \cdot \exp \left[ \int_0^{H_{stat}} \frac{-J_{d,lim}(-\alpha) + \mu_{rev}(\alpha)}{J_{d,lim}(\alpha) + J_{d,lim}(-\alpha)} d\alpha \right], \quad (9)$$

where  $\dot{J}_{d,lim}(\alpha) = dJ_{d,lim}(\alpha)/d\alpha$  is the slope of the descending branch of the experimental *limit cycle*,  $-H_{M,sat} \leq H_{stat} \leq H_{M,sat}$ , and  $\mu_{rev}$  is the reversible permeability of the material.

### 1) Calculation of the hysteresis loss component

The hysteresis loss component associated with the cycle taken between  $H_m$  and  $H_M$  is calculated as

$$W_{hyst}(H_M, H_m) = \oint_{\text{cycle}} H_{stat} dJ = \int_{H_m}^{H_M} H_{stat} \left( \frac{dJ_a}{dH_{stat}} - \frac{dJ_d}{dH_{stat}} \right) dH_{stat}, \quad (10)$$

where the slopes of the ascending and descending branches are introduced. By further introducing the quantity  $\varphi = d\Phi(H_{stat})/dH_{stat}$ , we obtain from (6)

$$\frac{dJ_d}{dH_{stat}} = 2\varphi(-H_{stat}) [\Phi(H_{stat}) - \Phi(H_M)] \quad (11)$$

and

$$\frac{dJ_a}{dH_{stat}} = 2\varphi(H_{stat}) [\Phi(H_{stat}) - \Phi(H_m)] \quad (12)$$

for the descending and ascending branch, respectively. Eq. (10) can then be written as

$$W_{hyst} = \int_{H_m}^{H_M} H_{stat} \cdot \left\{ 2\varphi(H_{stat}) [\Phi(H_{stat}) - \Phi(H_m)] - 2\varphi(-H_{stat}) [\Phi(H_{stat}) - \Phi(H_M)] \right\} dH_{stat}, \quad (13)$$

thereby providing a formal expression for the hysteresis loss component.

### 2) Calculation of the excess loss component

The excess loss component is derived from (5) as

$$W_{exc} = \int_0^{1/f} H_{exc} \dot{J} dt = \int_0^{1/f} \frac{4}{3} \sqrt{\frac{dH_{stat}}{dJ}} \cdot |J|^{3/2} dt, \quad (14)$$

where the term  $dH_{stat}/dJ$  is the inverse of the local slope of the static hysteresis loop. Recalling the expression (3) for  $W_{exc}$  provided by the STL and comparing it with (14), the statistical parameter  $V_0$ , lumping the effect of the local coercive fields in the STL, is obtained as

$$V_0(J_p, J_b) = \frac{1}{\sigma GS} \left( \frac{1}{T} \int_0^T \frac{4}{3} \sqrt{\frac{dH_{\text{stat}}}{dJ}} / k_d dt \right)^2. \quad (15)$$

In this derivation we have assumed, without loss of generality, that the statistical parameter  $V_0$  depends only on the bias polarization  $J_b$  and the peak-to-peak swing  $2J_p$ , while being independent on the induction waveform. This permits one to simplify the calculation by assuming a triangular  $J(t)$ .

In order to perform the integration (15) as a function of the variable  $H_{\text{stat}}$ , we decompose the cycle into the ascending and the descending branches and after some mathematics we obtain

$$V_0(J_p, J_b) = \frac{1}{9\sigma GS k_d J_p^2} \left[ \int_{H_m}^{H_M} \left( \sqrt{\frac{dJ_a}{dH_{\text{stat}}}} + \sqrt{\frac{dJ_d}{dH_{\text{stat}}}} \right) dH_{\text{stat}} \right]^2. \quad (16)$$

Introducing then (11) and (12) in (16), we get

$$V_0(J_p, J_b) = \frac{1}{9\sigma GS k_d J_p^2} \left( \int_{H_m}^{H_M} \left\{ \sqrt{2\varphi(H_{\text{stat}}) [\Phi(-H_{\text{stat}}) - \Phi(-H_m)] + \mu_{\text{rev}}(H_{\text{stat}})} \right. \right. \\ \left. \left. + \sqrt{2\varphi(-H_{\text{stat}}) [\Phi(H_{\text{stat}}) - \Phi(H_M)] + \mu_{\text{rev}}(H_{\text{stat}})} \right\} dH_{\text{stat}} \right)^2 \quad (17)$$

To simplify the whole matter, one might emulate the *limit cycle* by an analytical expression and make explicit the function  $\Phi$  and its derivative  $\varphi$ . Typically, a hyperbolic tangent expression does provide a good description of the *limit cycle* [37] and the descending branch of the *limit cycle* is correspondingly obtained as

$$J_d(H_{\text{stat}}) = A_0 \tanh \frac{H_{\text{stat}} + H_C}{\varsigma H_C} + \mu_{\text{rev}} \cdot H_{\text{stat}}, \quad (18)$$

with  $A_0$ ,  $H_C$ ,  $\varsigma$ , and  $\mu_{\text{rev}}$  fitting parameters. Combining (18) and (9) we get

$$\Phi(H_{\text{stat}}) = \frac{\sqrt{A_0 \tanh(1/\varsigma) \cdot \cosh(1/\varsigma)}}{\cosh\left(\frac{H_{\text{stat}} - H_C}{\varsigma H_C}\right)} \frac{\exp\left(-\frac{(1/\varsigma)}{\tanh(2/\varsigma)}\right)}{\exp\left(\frac{H_{\text{stat}} - H_C}{\varsigma H_C \tanh(2/\varsigma)}\right)} \quad (19)$$

and after derivation

$$\varphi(H_{\text{stat}}) = \frac{1}{\varsigma H_C \sinh(2/\varsigma)} \frac{\cosh\left(\frac{H_{\text{stat}} + H_C}{\varsigma H_C}\right)}{\cosh\left(\frac{H_{\text{stat}} - H_C}{\varsigma H_C}\right)} \Phi(H_{\text{stat}}). \quad (20)$$

By introducing the so-obtained  $\Phi(H_{\text{stat}})$  and  $\varphi(H_{\text{stat}})$  in (13) and (17), the hysteresis loss  $W_{\text{hyst}}$  and the excess loss  $W_{\text{exc}}$  (via (3)) can be numerically calculated. To remark that if a fitting formula for the *limit* experimental cycle different from (18) is assumed, the expressions (19) and (20) for the functions  $\Phi$  and  $\varphi$  are modified, but those for  $W_{\text{hyst}}$  and  $V_0$  remain valid.

### III. EXPERIMENTAL RESULTS

We discuss now two examples of validation of the discussed predictive model based on experiments performed on non-oriented Fe-Si sheets of thickness  $d = 0.194$  mm, and grain-oriented Fe-Si laminations of thickness  $d = 0.28$  mm.

#### A. Practical implementation of the model

Let us take the case where a hysteresis loop of peak-to-peak amplitude  $2J_p$  is measured under bias polarization of value  $J_b$ . In order to apply (13) and (17) and arrive at  $W_{\text{hyst}}$  and  $V_0$ , we need to determine the static fields  $H_m$  and  $H_M$  permitting one to reach the polarization levels  $J_b - J_p$  and  $J_b + J_p$ , respectively. This might be quite a complex problem, because one should take into account the magnetic history of the material prior to the moment where the biased cycle is executed. In practical applications, no information is typically available regarding such a history and a numerical inversion of the static hysteresis model is required. A simpler strategy is therefore adopted here, in order to approximately determine  $H_m$  and  $H_M$ , which consists in determining the anhysteretic magnetization curve, identified with the single valued  $J(H)$  curve intermediate between the ascending and descending branches of a major hysteresis loop. This  $J(H)$  can be inverted quite easily, in order to derive  $H_m$  and  $H_M$  from the peak polarization values  $J_b - J_p$  and  $J_b + J_p$ , as illustrated in Fig. 3. In conclusion, only the major hysteresis loop of the material is required by the model, in order to proceed with the identification process and for achieving the anhysteretic  $J(H)$  curve. A flow chart on the model implementation is given in Fig. 4.

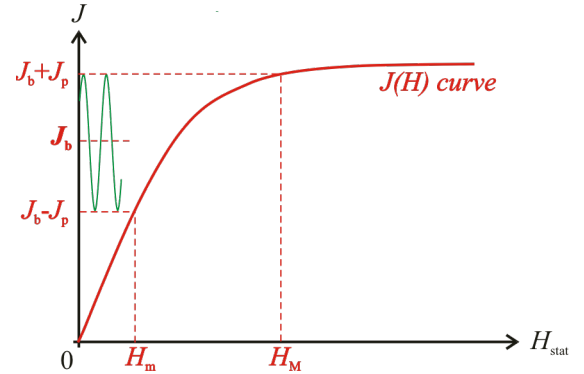


Fig. 3. Determination of the fields  $H_m$  and  $H_M$  corresponding to the lower  $J_b - J_p$  and upper  $J_b + J_p$  polarization values, respectively.

#### B. Model identification

##### 1) "Static" parameters

According to (19) and (20), the previously introduced parameters  $A_0$ ,  $H_C$ ,  $\varsigma$ , and  $\mu_{\text{rev}}$  need to be retrieved in order to calculate the  $\Phi$  and  $\varphi$  functions. Their values are obtained by fitting the descending branch of the major static hysteresis loop by (18). This operation provides for the NO sheets the values:  $A_0 = 1.33$  T,  $H_C = 39.4$  A/m,  $\varsigma = 1.1$ , and  $\mu_{\text{rev}} = 150 \cdot \mu_0$ . The measured conductivity of this Fe-Si alloy is  $\sigma = 1.99 \cdot 10^6$  S·m<sup>-1</sup>.



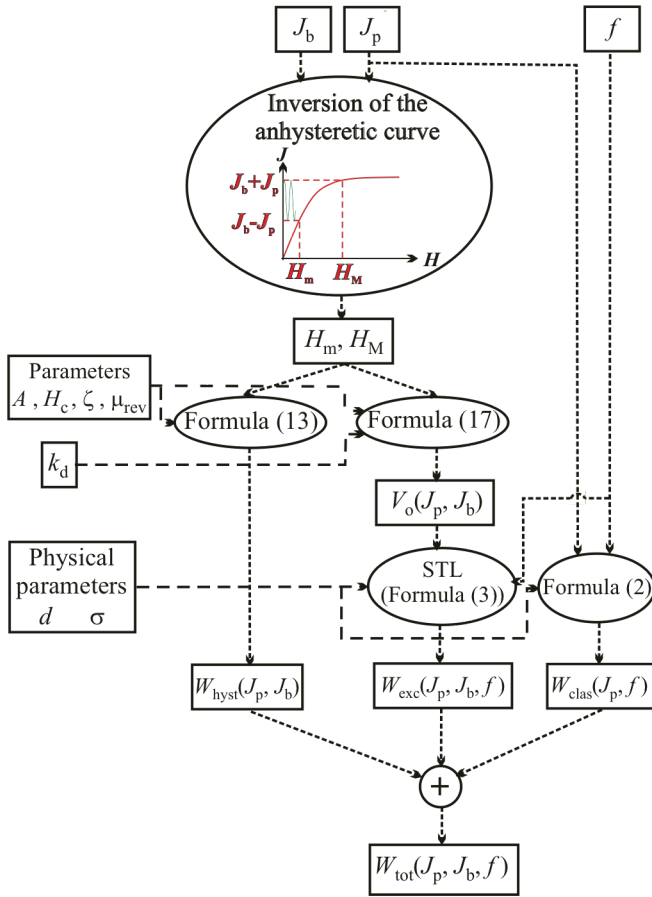


Fig. 4. Flow chart of the model implementation.

## 2) Derivation of the dynamic constant $k_d$

The constant  $k_d$  is related to the function  $V_0(J_p, J_b = 0)$ , which can be determined by the conventional loss separation (3), according to the STL, on symmetric loops ( $J_b = 0$ ) [17]. Once the curve  $V_0(J_p, J_b = 0)^{1/2} \cdot J_p^{3/2}$  is obtained in this way, calculation of  $V_0(J_p, J_b = 0)$  is made by (17) and the value of the constant  $k_d$  providing best fitting of the curve is retained. Fig. 5. illustrates such a fitting (least squares algorithm), providing the value of the dynamic constant  $k_d = 1200 \text{ mA}^{-1} \text{ s}^{-1}$ . To sum up the identification procedure, a flow chart is given in Fig. 6.

## C. Experiments

### 1) Experimental procedure

Measurements on NO sheets have been performed with and without DC bias up to 1000 Hz, below the frequency range where the skin effect is likely to appear [31]. A 700-turn Epstein frame has been employed up to 400 Hz, substituted by a 200-turn frame at higher frequencies. Unambiguous measurements can be performed without DC bias and do not need detailed discussion here. Specifications are instead required for the DC-biased measurements, because several options regarding the way the experiments are performed are possible, according to the magnetic history of the material. In [34] the sample is, for example, brought to the saturated state and the minor loop is run along the descending branch of the major cycle. In the present experiments, the sample has been

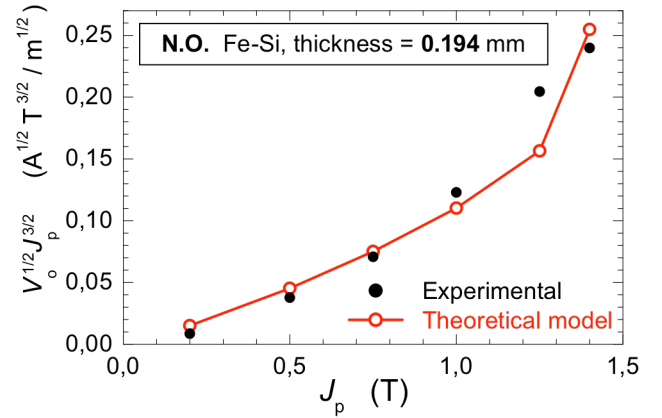


Fig. 5. Behavior of the quantity  $(V_0)^{1/2} \cdot J_p^{3/2}$  versus  $J_p$  with centered hysteresis loops in the NO 0.194 mm thick Fe-Si sheet. The results obtained by conventional loss separation procedure (experimental) are compared with the prediction of (17) using best fitting value of the dynamic constant  $k_d$ .

carefully demagnetized at a low frequency before applying the DC bias. As shown in Fig. 7, the DC-biased cycle, of frequency  $f = 1/T$ , is nested inside a major symmetric loop of period equal to  $10T$ . The acquisition of the specific DC-biased cycle is carried out at the end of the positive half-period of the major cycle. Before acquisition, a number of identically DC-biased cycles are made in order to reach steady state (it was shown in [34] that a few cycles are required before reaching a stable periodic behavior of the minor loop).

## 2) Results

A peak polarization  $J_p = 0.5 \text{ T}$  has been chosen, and three different values of DC bias have been considered:  $J_b = 0 \text{ T}$  (centered case),  $J_b = 0.5 \text{ T}$ , and  $J_b = 0.75 \text{ T}$ . A conventional loss separation procedure is performed, by which the experimental excess loss  $W_{exc}$  is obtained by subtracting the measured hysteresis loss and the classical loss components

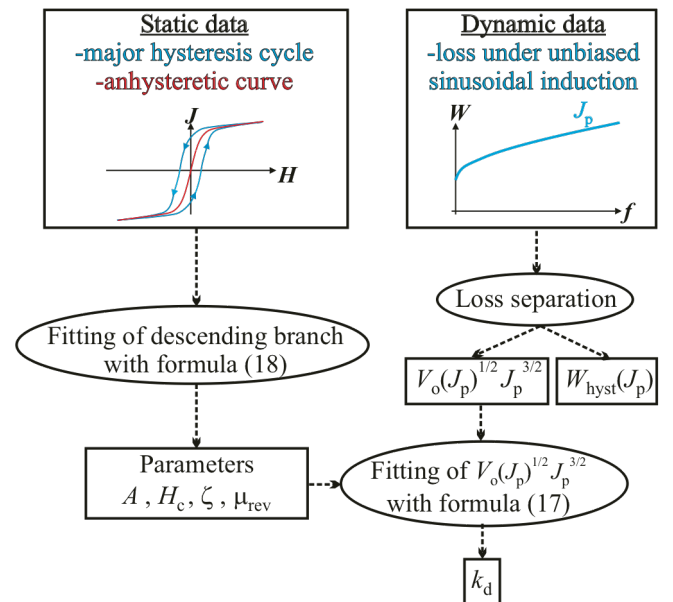


Fig. 6. Flow chart of the identification procedure, by which the parameters  $A$ ,  $H_c$ ,  $\zeta$ ,  $\mu_{rev}$ , and  $k_d$  are obtained from the static and dynamic data.

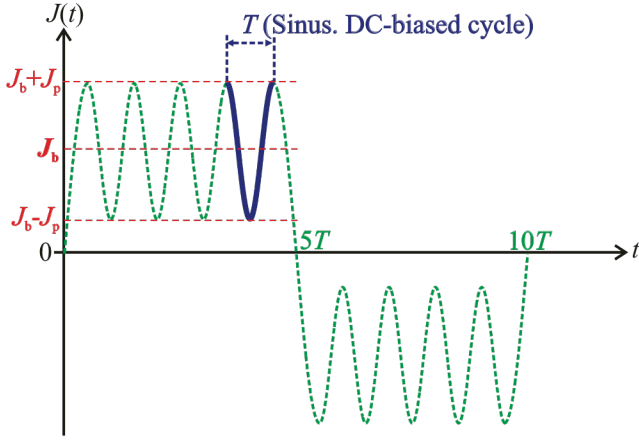


Fig. 7. Application of the DC-biased polarization waveform.

from the measured energy loss (symbols in Fig. 8a). The value of the parameter  $V_0(J_p, J_b)$  is then obtained by (16) and the excess loss is calculated with (3) (lines in Fig. 8a). It is found that the increase of the slope of the experimental  $W_{\text{exc}}(f)$  versus  $f^{1/2}$  behavior is correctly taken into account by the function  $V_0(J_p, J_b)$ . Fig.8b shows the behavior of the measured loss

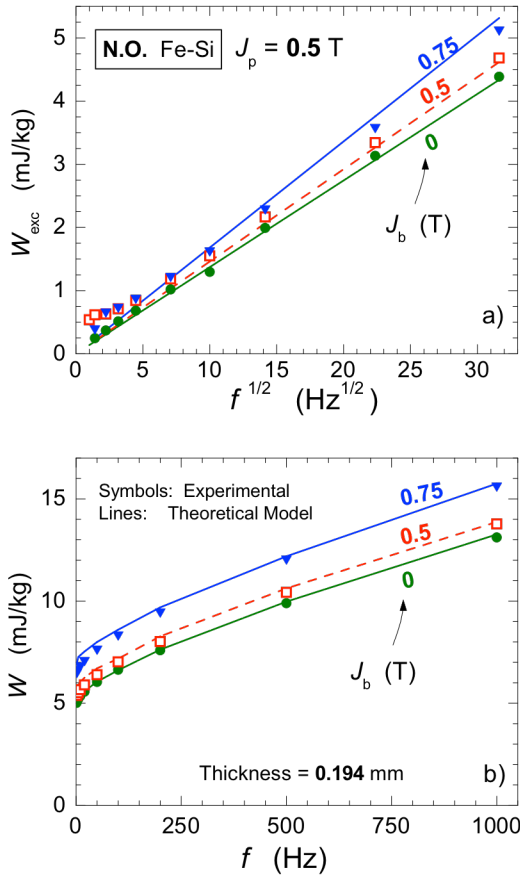


Fig. 8 Non-oriented Fe-Si 0.194 mm thick sheet under sinusoidal induction waveform ( $J_p = 0.5$  T;  $J_b = 0$ ,  $J_b = 0.5$  T, and  $J_b = 0.75$  T). Experimental values and outcomes of the proposed theoretical model are compared vs. frequency. a) Excess loss  $W_{\text{exc}}$ . b) Total loss  $W$ .

(symbols) and the predicted one (lines) obtained by adding the classical loss (2), the previously calculated  $W_{\text{exc}}(f)$ , and the hysteresis loss  $W_{\text{hyst}}$  calculated with (13). Neglecting the DC bias can lead to significant errors: for example, for a bias of 0.75 T, the loss at 100 Hz is  $\sim 23\%$  greater than the value obtained for unbiased conditions.

### 3) Validation on grain-oriented Fe-Si sheets

An advantage of this material is its relatively important permeability, making it easier to reach higher polarization levels than in NO sheets. The GO sheets are also characterized by wide domain wall spacing, the source of a remarkable excess loss contribution, and provide a significant applicative example of the model. The same peak-to-peak induction of  $2 \cdot J_p = 1$  T has been considered, and DC bias up to  $J_b = 1.2$  T has been reached. The previously described identification procedure provides the following parameters:  $A_0 = 1.87$  T,  $H_C = 6.8$  A/m,  $\zeta = 0.5$ , and  $\mu_{\text{rev}} = 200 \cdot \mu_0$ . The conductivity is  $\sigma = 2.08 \cdot 10^6$  S·m<sup>-1</sup>. The dynamic constant has been found equal to  $k_d = 57$  mA·s<sup>-1</sup>. The results, showing a satisfying agreement with the theory, are given in Fig. 9.

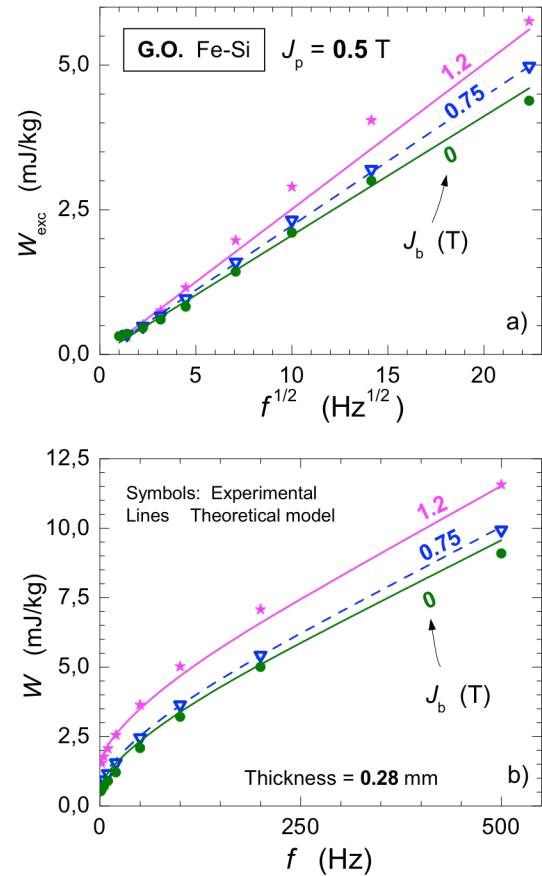


Fig. 9. Grain-oriented Fe-Si 0.28 mm thick sheets under sinusoidal induction waveform ( $J_p = 0.5$  T;  $J_b = 0$ ,  $J_b = 0.75$  T, and  $J_b = 1.2$  T). Experimental and theoretical loss vs. frequency: a) Excess loss  $W_{\text{exc}}$ ; b) Total loss  $W$ .

## IV. CONCLUSION

In this article, the importance of DC-biased loops in applications has been highlighted. A simple computational scheme, based on the extension of the Statistical Loss Theory to DC-biased waveforms, has been proposed. Semi-analytical formulae have been derived for the hysteresis contribution, and the  $V_0$  parameter of the Statistical Theory of Losses. The model requires acquisition and fitting of the major symmetric static hysteresis loop, and the identification of a single constant  $k_d$  governing the dynamic magnetization process. This dynamic constant is obtained by fitting the statistical parameter  $V_0(J_p)$  experimentally found with unbiased sinusoidal induction. Two examples of application of the theoretical model, regarding 0.194 mm thick non-oriented and 0.28 mm thick grain-oriented Fe-Si sheets, have been discussed. Measurements performed under DC-bias are shown to be in good agreement with the prediction, both regarding the excess loss and the hysteresis loss components. This model appears then to provide a computationally simple predicting tool for electrical engineers facing the problem of DC-biased regimes, relieving the designer from the quest for cumbersome measurements under polarized induction.

## REFERENCES

- [1] A. S. Abdel-Khalik, S. Ahmed, A. M. Massoud, and A. A. Elserougi, "An improved performance direct-drive permanent magnet wind generator using a novel single-layer winding layout," *IEEE Trans. Magn.*, vol. 49, DOI 10.1109/TMAG.2013.2257823, no. 9, pp. 5124–5134, Sept. 2013.
- [2] Won-Ho Kim, Mi-Jung Kim, Ki-Doek Lee, Jae-Jun Lee, Jung-Ho Han, Tae-Chul Jeong, Su-Yeon Cho, Ju Lee, "NE-Map-Based Design of an IPMSM for Traction in an EV," *IEEE Trans. Magn.*, vol. 50, DOI 10.1109/TMAG.2013.2273827, no. 1, article number 4001404, Jan. 2014.
- [3] Wei Hua, Xiaomei, Yin, Gan Zhang, and Ming Cheng, "Analysis of Two Novel Five-Phase Hybrid-Excitation Flux-Switching Machines for Electric Vehicles," *IEEE Trans. Magn.*, vol. 50, DOI 10.1109/TMAG.2014.2323089, no. 11, article number 8700305, Nov. 2014.
- [4] Mi-Jung Kim, Su-Yeon Cho, Ki-Doek Lee, Jae-Jun Lee, Jung-Ho Han, Tae-Chul Jeong, Won-Ho Kim, Dae-Hyun Koo, Ju Lee, "Torque density elevation in concentrated winding interior PM synchronous motor with minimized magnet volume," *IEEE Trans. Magn.*, vol. 49, DOI 10.1109/TMAG.2013.2241747, no. 7, pp. 3334–3337, July 2013.
- [5] J. H. Lee and B. I. Kwon, "Optimal rotor shape design of a concentrated flux IPM-type motor for improving efficiency and operation range," *IEEE Trans. Magn.*, vol. 49, DOI 10.1109/TMAG.2013.2242458, no. 5, pp. 2205–2208, May 2013.
- [6] J. Pippuri, A. Manninen, J. Keranen, and K. Tammi, "Torque density of radial, axial and transverse flux permanent magnet machine topologies," *IEEE Trans. Magn.*, vol. 49, DOI 10.1109/TMAG.2013.2238520, no. 5, pp. 2339–2342, May 2013.
- [7] L. D. S. Coelho, V. C. Mariani, F. A. Guerra, M. V. da Luz, and J. V. Leite, "Multiobjective optimization of transformer design using a chaotic evolutionary approach," *IEEE Trans. Magn.*, vol. 50, DOI 10.1109/TMAG.2013.2285704, no. 2, article number 7016504, pp. 669–672, Feb. 2014.
- [8] S. L. Ho, S. Yang, G. Ni, and J. Huang, "A quantum-based particle swarm optimization algorithm applied to inverse problems," *IEEE Trans. Magn.*, vol. 49, DOI 10.1109/TMAG.2013.2237760, no. 5, pp. 2069–2072, May 2013.
- [9] B. Xia, M. T. Pham, Y. Zhang, and C. S. Koh, "A global optimization algorithm for electromagnetic devices by combining adaptive Taylor Kriging and particle swarm optimization," *IEEE Trans. Magn.*, vol. 49, DOI 10.1109/TMAG.2013.2238907, no. 5, pp. 2061–2064, May 2013.
- [10] Dong-Kuk Lim, Dong-Kyun Woo, Il-Woo Kim, Jong-Suk Ro, Hyun-Kyo Jung, "Cogging torque minimization of a dual-type axial-flux permanent magnet motor using a novel optimization algorithm," *IEEE Trans. Magn.*, vol. 49, DOI 10.1109/TMAG.2013.2256430, no. 9, pp. 5106–5111, Sept. 2013.
- [11] Zbigniew Gmyrek, Aldo Boglietti, and Andrea Cavagnino, "Estimation of Iron Losses in Induction Motors: Calculation Method, Results, and Analysis," *IEEE Trans. Ind. Electron.*, vol. 57, DOI 10.1109/TIE.2009.2024095, no. 1, pp. 161–171, Jan. 2010.
- [12] K. Komeza, M. Doms, "Finite-Element and Analytical Calculations of No-Load Core Losses in Energy-Saving Induction Motors," *IEEE Trans. Ind. Electron.*, vol. 59, DOI 10.1109/TIE.2011.2168795, no. 7, pp. 2934–2946, July 2012.
- [13] Sa Zhu, Ming Cheng, "Core Loss Analysis and Calculation of Stator Permanent-Magnet Machine Considering DC-Biased Magnetic Induction," *IEEE Trans. Ind. Electron.*, vol. 61, DOI 10.1109/TIE.2014.2300062, no. 10, pp. 5203–5212, Oct. 2014.
- [14] O. Bottauscio, A. Canova, M. Chiampi, and M. Repetto, "Iron losses in electrical machines: influence of different material models," *IEEE Trans. Magn.*, vol. 38, DOI 10.1109/20.996208, no. 2, pp. 805–808, Mar. 2002.
- [15] M. LoBue, F. Mazaleyrat, and V. Loyau, "Study of magnetic losses in Mn-Zn ferrites under biased and asymmetric excitation waveforms," *IEEE Trans. Magn.*, vol. 46, DOI 10.1109/TMAG.2009.2031471, no. 2, pp. 451–454, Feb. 2010.
- [16] P. Markatos, J. P. Hall, and S. E. Zirka, "Power Loss Measurement and Prediction of Soft Magnetic Powder Composites Magnetized Under Sinusoidal and Nonsinusoidal Excitation," *IEEE Trans. Magn.*, vol. 44, DOI 10.1109/TMAG.2008.2001321, no. 11, pp. 3847–3850, Nov. 2008.
- [17] E. Barbisio, F. Fiorillo, and C. Ragusa, "Predicting Loss in Magnetic Steels Under Arbitrary Induction Waveform and With Minor Hysteresis Loops," *IEEE Trans. Magn.*, vol. 40, DOI 10.1109/TMAG.2004.830510, no. 4, pp. 1810–1819, July 2004.
- [18] M. Hafner, T. Finken, M. Felden, and K. Hameyer, "Automated Virtual Prototyping of Permanent Magnet Synchronous Machines for HEVs," *IEEE Trans. Magn.*, vol. 47, DOI 10.1109/TMAG.2010.2091675, no. 5, pp. 1018–1021, May 2011.
- [19] K. Atallah, D. Howe, P. H. Mellor, and D. A. Stone, "Rotor loss in permanent-magnet brushless AC machines," *IEEE Trans. Ind. Appl.*, vol. 36, DOI 10.1109/28.887213, no. 6, pp. 1612–1618, Nov./Dec. 2000.
- [20] O. Bottauscio, G. Pellegrino, P. Guglielmi, M. Chiampi, and A. Vagati, "Rotor Loss Estimation in Permanent Magnet Machines With Concentrated Windings," *IEEE Trans. Magn.*, vol. 41, DOI 10.1109/TMAG.2005.854969, no. 10, pp. 3913–3915, Oct. 2005.
- [21] Andreas Krings, "Iron Losses in Electrical Machines — Influence of Material Properties, Manufacturing Processes, and Inverter Operation," Doctoral Thesis, KTH School of Electrical Engineering, Stockholm, Sweden, April 2014.
- [22] T. V. Tran, F. Moussouni, S. Brisset, and P. Brochet, "Adapted output space-mapping technique for a bi-objective optimization," *IEEE Trans. Magn.*, vol. 46, DOI 10.1109/TMAG.2010.2043343, no. 8, pp. 2990–2993, Aug. 2010.
- [23] J. Li, T. Abdallah, and C. R. Sullivan, "Improved calculation of core loss with nonsinusoidal waveforms," in *36<sup>th</sup> Industry Applications Conference (IAS)*, vol. 4, DOI 10.1109/IAS.2001.955931, Oct. 2001, pp. 2203–2210.
- [24] S. Okazaki, Y. Asano, T. Yanase, "AC magnetic properties of electrical steel core under DC-biased magnetization," *Journal of Magnetism and Magnetic Materials*, vol. 215–216, pp. 156–158, June 2000.
- [25] M. Enokizono and Y. Takeshima, "Measurement system of alternating magnetic properties under DC-biased field," *Journal of Magnetism and Magnetic Materials*, vol. 215–216, pp. 704–707, June 2000.
- [26] S. Zhu, M. Cheng, J. Dong, and J. Du, "Core Loss Analysis and Calculation of Stator Permanent-Magnet Machine Considering DC-Biased Magnetic Induction," *IEEE Trans. Ind. Electron.*, vol. 61, DOI 10.1109/TIE.2014.2300062, no. 10, pp. 5203–5212, Oct. 2014.
- [27] G. Bertotti, "Dynamic generalization of the scalar Preisach model of hysteresis," *IEEE Trans. Magn.*, vol. 28, DOI 10.1109/20.179569, no. 5, pp. 2599–2601, Sep. 1992.
- [28] V. Basso, G. Bertotti, O. Bottauscio, F. Fiorillo, M. Pasquale, M. Chiampi, and M. Repetto, "Power losses in magnetic laminations with hysteresis: Finite element modeling and experimental validation," *J. Appl. Phys.*, vol. 81, DOI 10.1063/1.364614, pp. 5606–5608, April 1997.
- [29] O. Bottauscio, M. Chiampi, and D. Chiarabaglio, "Advanced model of laminated magnetic cores for two-dimensional field analysis," *IEEE*



*Trans. Magn.*, vol. 36, DOI 10.1109/20.846219, no. 3, pp. 561–573, May 2000.

- [30] O. de la Barrière, C. Ragusa, C. Appino, F. Fiorillo, M. LoBue, F. Mazaleyrat, “A computationally effective dynamic hysteresis model taking into account skin effect in magnetic laminations,” *Physica B: Condensed Matter*, vol. 435, pp. 80–83, Feb. 2014.
- [31] C. Beatrice, C. Appino, O. de la Barrière, F. Fiorillo, and C. Ragusa, “Broadband Magnetic Losses in Fe-Si and Fe-Co Laminations,” *IEEE Trans. Magn.*, vol. 50, DOI 10.1109/TMAG.2013.2286923, no. 4, article number 6300504, April 2014.
- [32] Giorgio Bertotti, *Hysteresis in Magnetism*. San Diego, California: Academic Press, May 1998.
- [33] G. Bertotti, “General properties of power losses in soft ferromagnetic materials,” *IEEE Trans. Magn.*, vol. 24, DOI 10.1109/20.43994, no. 1, pp. 621–630, Jan. 1988.
- [34] E. Barbisio, O. Bottauscio, M. Chiampi, and C. Ragusa, “Analysis of AC magnetic properties in SiFe laminations under DC-biased magnetisation,” *Physica B: Condensed Matter*, vol. 343, no. 1–4, pp. 127–131, Jan. 2004.
- [35] E. Barbisio, O. Bottauscio, M. Chiampi, F. Fiorillo, and C. Ragusa, “Prediction of magnetic power losses in soft laminations under DC-biased supply,” *Journal of Magnetism and Magnetic Materials*, vol. 290–291, Part 2, pp. 1476–1479, Apr. 2005.
- [36] C. Ragusa, “An analytical method for the identification of the Preisach distribution function,” *Journal of Magnetism and Magnetic materials*, vol. 254–255, pp. 259–261, Jan. 2003.
- [37] C. Ragusa, “Analytical expressions of Preisach distribution function,” in *IEEE International Magnetism Conference (INTERMAG Europe)*, DOI 10.1109/INTMAG.2002.1001346, May 2002, p. FS3.



**Olivier de la Barrière** was born in Paris, France, in 1982. He received the M.S. and PhD degrees in Electrical Engineering from the Ecole Normale Supérieure de Cachan, Cachan, France, in 2007 and 2010, respectively. He has been full time CNRS researcher at SATIE laboratory, Cachan, France since 2012. He was post-doctoral scientist at the National Institute of for Research in Metrology (INRiM), Torino, Italy, in 2011-2012. His research

interests are focused on electrical machine design, axial flux machines, and iron loss measurement and modeling in soft magnets.

Dr. de la Barrière has been member of the Steering Committee of the Advances in Magnetism Conference (AIM), Bormio, Italy, 2016.



**Carlo Ragusa** (M'15) was born in Catania, Italy. He received the M.Sc. degree in electrical engineering from the University of Catania, Catania, Italy, in 1993 and the PhD in electrical engineering from Politecnico di Torino, Torino, Italy, in 1997.

He has been Associate Professor of Electrical Engineering at Energy Department – Politecnico di Torino, Torino, Italy since 2005. In 2010 and 2014 he was Invited Professor at École Normale

Supérieure de Cachan, France. His research interests focus on experimental characterization and modelling of soft magnets, computational electromagnetics, and numerical micromagnetics.

Prof. Ragusa has been member of the International Organizing Committee of the Soft Magnetic Materials Conference since 2015, and member of the Steering Committee of the International Workshop on 1&2 Dimensional Magnetic Measurement and Testing since 2012. He served as Editor for the Soft Magnetic Materials Conference in 2009 and 2015.



**Carlo Appino** was born in Biella, Italy in 1961. He received the degree in physics from the Università di Torino (Italy) in 1985, and the doctoral degree in physics from the Politecnico di Torino in 1992.

He has been Researcher at Istituto Nazionale di Ricerca Metrologica, Torino, since 1994. He was Invited Researcher at the CNRS of Grenoble (France), and at the ENS of Cachan (France). His research activity has been

mainly devoted to theoretical and experimental investigation of soft magnets, with particular reference to hysteresis phenomena in amorphous and crystalline materials, soft magnetic composites, and vector magnetization process.

Dr. Appino has been member of the Steering Committee of the International Workshop on 1&2 Dimensional Magnetic Measurement and Testing (2DM) since 2014. He served as Editor for the International Conference on Magnetism in 2003, for the 2DM in 2014, and for the Soft Magnetic Materials Conference in 2009 and 2015.



**Fausto Fiorillo** was born in Bricherasio, Italy. He received the Doctor degree in physics from University of Torino, Italy, in 1972.

He was Research Director, till his retirement in 2012, at the Istituto Nazionale di Ricerca Metrologica (INRiM) in Torino (formerly Istituto Elettrotecnico Nazionale Galileo Ferraris), where he is pursuing at present research studies in magnetism as an associate scientist.

He authored/co-authored some 200 peer-reviewed publications in international scientific journals, review monographs, and chapters on international series on magnetic materials and is the author of the comprehensive treatise “*Measurement and Characterization of Magnetic Materials*” (10 Chapters, 647 pages), published by Academic Press-Elsevier, December 2004.

Dr. Fiorillo served as Chairman of the International Organizing Committee of the Soft Magnetic Materials Conference from 1993 through 2001.